Proceedings of the 2006 IEEE
International Conference on Robotics and Biomimetics
December 17 - 20, 2006, Kunming, China

Impedance Control of the Hydraulic Shoulder
A 3-DOF Parallel Manipulator

H. Sadjadian and **H. D. Taghirad**[†]
Advanced **R**obotics and **A**utomated **S**ystems (**ARAS**)
Department of Electrical Engineering
K.N. Toosi University of Technology
[†]Taghirad@kntu.ac.ir

Abstract – **In this paper, a model-based impedance control strategy is developed for a 3 DOF parallel manipulator to manage the interaction of the robot with the environment. Kinematic and dynamic modeling of the manipulator has been analyzed in order to be used for both simulation and control purposes. The impedance controller objective and the structure of the proposed controller are introduced and controller gain selection is discussed. A simulation study evaluates the effectiveness of the proposed impedance control structure. It is observed that although the proposed controller is designed for impedance adjustment of the robot, in case of free motion, it results into desirable position tracking. Moreover, when the robot comes into contact with the environment, the interaction dynamics can be regulated regardless of the nonlinear dynamics of the robot.**

Index Terms – Parallel manipulator, impedance control, model-based control, stiff environment.

I. INTRODUCTION

Over the last two decades, parallel manipulators have been among the most considerable research topics in the field of robotics. A parallel manipulator typically consists of a moving platform that is connected to a fixed base by several limbs. The number of limbs is at least equal to the number of degrees of freedom (DOF) of the moving platform so that each limb is driven by no more than one actuator, and all actuators can be mounted on or near the fixed base. These robots are now used in real-life applications such as force sensing robots, fine positioning devices, and medical applications [1, 2].

When a manipulator is in contact with a constraining surface which is generally called as the environment, force is generated between the manipulator end effector and the environment. The amount of the force exerted by the manipulator on the environment depends on how much the end effector position is physically constrained by the environment to reach its goal position. Hence, the contact force can be regulated by appropriate control of the end effector position. In literature, a variety of approaches have been proposed that allow position and force control in different manipulation tasks [3], especially where a relatively permanent contact of the manipulator with the environment is needed.

Perhaps the most straightforward control approach in such tasks is the Hybrid approach, also known as Hybrid interaction control. In this approach, Cartesian or task axes are separated into constrained and unconstrained axes and position and force are controlled separately in their own controllable directions, where position control is performed along unconstrained and force control is performed along constrained directions.

Another most frequently used approach considers a certain desired dynamic specification of the manipulator behavior, well-known as the manipulator impedance which describes the dynamic relationship between positions and forces or equivalently between orientations and torques. In this impedance control approach the robot end effector position is adjusted in response to the sensed contact force in such a way that a target impedance relationship is satisfied. In this way, under an external force, the manipulator must behave as the desired impedance, tracking the target referenced trajectory. The impedance concept was proposed first in [4] in order to avoid large values of contact forces and moments due to the robot/environment interaction. This is achieved by enforcing a compliant behavior of the end effector with suitable dynamic features, characterized by a desired inertia, damping and stiffness. A survey of interaction control schemes and comparison of different methods can be found in [5].

Parallel manipulators are attractive for tasks requiring the control of forces or moments because of their inherent stiffness. Many researchers consider the position control for parallel manipulators especially the Stewart platform. However, parallel manipulators with 3 DOF have been also implemented for applications where 6 DOF are not required, such as high-speed machine tools. Recently, 3 DOF parallel manipulators with more than three limbs have been investigated, in which the additional limbs separate the function of actuation from that of constraints at the cost of increased mechanical complexity [6]. Position control of such mechanisms has not received much attention so far and is still regarded as an interesting problem in parallel robotics research. Furthermore, regarding the developing field of parallel manipulator control, it is crucial to consider the control of forces as the manipulator is in contact with the environment while undergoing a constraint motion. Hybrid control has been applied to parallel manipulators [7]. Impedance control techniques have also been used, in particular in haptic interfaces [7]. However, the literature on impedance control of parallel manipulators, especially for 3 DOF redundant mechanisms, is much limited than that of conventional serial manipulators.

In this paper, a model-based impedance control strategy is developed for a three DOF actuator redundant hydraulic parallel manipulator to manage the interaction of the robot with the environment. The paper is organized as following. Section 2 contains the mechanism description, while kinematics modeling of the mechanism is studied in section 3.

In section 4 dynamic formulation of the manipulator is discussed as a key element in model based control design. The proposed structure for impedance control of the manipulator is elaborated in section 5 and the results are analyzed using a simulation study.

II. MECHANISM DESCRIPTION

A schematic of the mechanism, which is currently under experimental studies in ARAS Robotics Lab, is shown in Fig. 1. The mechanism is originally designed by Vincent Hayward [8], borrowing design ideas from biological manipulators particularly the biological shoulder. The interesting features of this mechanism and its similarity to human shoulder have made its design unique, which can serve as the basis for a good experimental setup for parallel robot research. As shown in figure 1, the mobile platform is constrained to spherical motions. Four high performance hydraulic piston actuators are used to give three degrees of freedom in the mobile platform. Each actuator includes a position sensor of LVDT type and an embedded Hall Effect force sensor. The four limbs share an identical kinematic structure. A passive limb connects the fixed base to the moving platform by a spherical joint, which suppresses the pure translations of the moving platform. Simple elements like spherical and universal joints are used in the structure. A complete analysis of such a careful design will provide us with required characteristics regarding the structure itself, its performance, and the control algorithms.

From the structural point of view, the shoulder mechanism which, from now on, we call it "the Hydraulic Shoulder" falls into an important class of robotic mechanisms called parallel robots. The motivation behind using these types of robot manipulators was to compensate for the shortcomings of the conventional serial manipulators such as low precision, stiffness and load carrying capability. However, they have their own disadvantages, which are mainly smaller workspace and many singular configurations. The hydraulic shoulder, having a parallel structure, has the general features of these structures. It can be considered as a shoulder for a light weighed seven DOF robotic arm, which can carry loads several times its own weight. Simple elements, used in this design, add to its lightness and simplicity. The workspace of such a mechanism can be considered as part of a spherical surface. The orientation angles are limited to vary between -$\pi/6$ and $\pi/6$. No sensors are available for measuring the orientation angles of the moving platform which justifies the importance of the forward kinematic map as a key element in feedback position control of the shoulder with the LVDT position sensors used as the output of such a control scheme. In former studies by the authors, different numerical approaches have been used to solve the forward kinematic map of this manipulator [9]. Furthermore, complete kinematic modeling resulting in a closed-form forward kinematics solution, Jacobian analysis through a complete velocity analysis of the mechanism, and singularity analysis are all discussed in detail in [10].

III. HYDRAULIC SHOULDER KINEMATICS

Fig. 2 depicts a geometric model for the hydraulic shoulder manipulator which will be used for its kinematics derivation.

Figure 1. The Hydraulic Shoulder Manipulator

Two coordinate frames are defined for the purpose of analysis. The base coordinate frame $\{A\}: x_0y_0z_0$ is attached to the fixed base at point C (rotation center) with its z_0-axis perpendicular to the plane defined by the actuator base points $A_1A_2A_3A_4$ and an x_0-axis parallel to the bisector of angle $\angle A_1CA_4$. The second coordinate frame $\{B\}: x_4y_4z_4$ is attached to the center of the moving platform P with its z-axis perpendicular to the line defined by the actuators moving end points (P_1P_2) along the passive limb. Note that we have assumed that the actuator fixed endpoints lie on the same plane as the rotation center C. The position of the moving platform center P is defined by:

$$^{A}p = [p_x, p_y, p_z]^T \tag{1}$$

Also, a rotation matrix $^{A}R_B$ is used to define the orientation of the moving platform with respect to the base frame:

$$^{A}R_B = R_z(\theta_z)R_y(\theta_y)R_x(\theta_x) = \begin{bmatrix} c\theta_z c\theta_y & c\theta_z s\theta_y s\theta_x - s\theta_z c\theta_x & c\theta_z s\theta_y c\theta_x + s\theta_z s\theta_x \\ s\theta_z c\theta_y & s\theta_z s\theta_y s\theta_x + c\theta_z c\theta_x & s\theta_z s\theta_y c\theta_x - c\theta_z s\theta_x \\ -s\theta_y & c\theta_y s\theta_x & c\theta_y c\theta_x \end{bmatrix} \tag{2}$$

where $\theta_x, \theta_y, \theta_z$ are the orientation angles of the moving platform denoting rotations of the moving frame about the fixed x, y, and z axes respectively. Also $c\theta$ and $s\theta$ denote $\cos(\theta)$ and $\sin(\theta)$ respectively.

With the above definitions, the 4×4 transformation matrix $^{A}T_B$ is easily found to be:

$$^{A}T_B = \begin{bmatrix} ^{A}R_B & ^{A}p \\ \mathbf{0} & 1 \end{bmatrix} \tag{3}$$

Hence, the position and orientation of the moving platform are completely defined by six variables, from which, only three orientation angles $\theta_x, \theta_y, \theta_z$ are independently specified as the task space variables of the hydraulic shoulder.

The kinematic vector-loop equation for each actuated limb can be written as:

$$L_i = l_i.s_i = {}^{A}p + {}^{A}R_B\,{}^{B}p_i - a_i \tag{4}$$

where l_i is the length of the i^{th} actuated limb and s_i is a unit vector pointing along the direction of the i^{th} actuated limb. Also, ^{A}p is the position vector of the moving platform and $^{A}R_B$ is its rotation matrix. Vectors a_i and $^{B}p_i$ denote the fixed

end points of the actuators (A_i) in the base frame and the moving end points of the actuators respectively, written as:

$$a_1 = {}^{A}A_1 = \begin{pmatrix} l_b \sin\alpha & -l_b \cos\alpha & 0 \end{pmatrix}^T,$$
$$a_2 = {}^{A}A_2 = \begin{pmatrix} -l_b \sin\alpha & -l_b \cos\alpha & 0 \end{pmatrix}^T,$$
$$a_3 = {}^{A}A_3 = \begin{pmatrix} -l_b \sin\alpha & l_b \cos\alpha & 0 \end{pmatrix}^T, \quad (5)$$
$$a_4 = {}^{A}A_4 = \begin{pmatrix} l_b \sin\alpha & l_b \cos\alpha & 0 \end{pmatrix}^T,$$

and,

$$ {}^{B}p_1 = \begin{pmatrix} 0 & -l_d & -l_k \end{pmatrix}^T, \quad (6)$$
$$ {}^{B}p_2 = \begin{pmatrix} 0 & l_d & -l_k \end{pmatrix}^T.$$

Hence, the actuator lengths l_i can be easily computed by dot-multiplying (4) with itself to yield:

$$L_i^T . L_i = l_i^2 = [{}^{A}p + {}^{A}R_B \, {}^{B}p_i - a_i]^T [{}^{A}p + {}^{A}R_B \, {}^{B}p_i - a_i] \quad (7)$$

Writing (7) four times with the corresponding parameters given in (2), (5) and (6), and through algebraic simplifying, results in the complete kinematic model of the hydraulic shoulder.

For the Jacobian analysis of the Hydraulic shoulder, we must find a relationship between the angular velocity of the moving platform, $\boldsymbol{\omega}$, and the vector of limb rates as the actuator space variables, $\dot{\mathbf{l}} = \begin{bmatrix} \dot{l}_1 & \dot{l}_2 & \dot{l}_3 & \dot{l}_4 \end{bmatrix}^T$, so that:

$$\dot{\mathbf{l}} = J\boldsymbol{\omega} \quad (8)$$

From the above definition, it is easily observed that the Jacobian for the Hydraulic shoulder will be a 4×3 rectangular matrix as expected, regarding the mechanism as an actuator redundant manipulator. Using the idea of mapping between actuator, joint and task space, we find that the Jacobian depends on the actuated limbs as well as the passive supporting limb. Therefore, we first derive a 4×6 Jacobian, J_l, relating the six-dimensional velocity of the moving platform, $\mathbf{v}$, to the vector of actuated limb rates, $\dot{\mathbf{l}}$. Then, we find the 6×3 Jacobian of the passive supporting limb, J_p. The Jacobian of the Hydraulic shoulder will be finally derived as:

$$J = J_l J_p \quad (9)$$

The details of the expression of the Jacobians can be found in [10].

IV. Hydraulic Shoulder Dynamcis

In this section the dynamic model of the hydraulic shoulder is derived based on the application of the Lagrange formulation with θ chosen as the vector of generalized coordinates. The equation of motion can be written as:

$$\frac{d}{dt}\left(\frac{\partial L}{\partial \dot{\theta}}\right) - \frac{\partial L}{\partial \theta} = \tau_g \quad (10)$$

where the Lagrangian function $L = T - U$ is the difference between the kinetic energy T and the potential U of the system and τ_g is the vector of the generalized torques. The kinetic energy can be written by adding translational and rotational contributions as:

$$T = T(\theta, \dot{\theta}) = \frac{1}{2}\dot{\theta}^T M(\theta)\dot{\theta} \quad (11)$$

where $\theta \in R^3$ and $M \in R^{3\times3}$. Similarly, the potential energy can be written as:

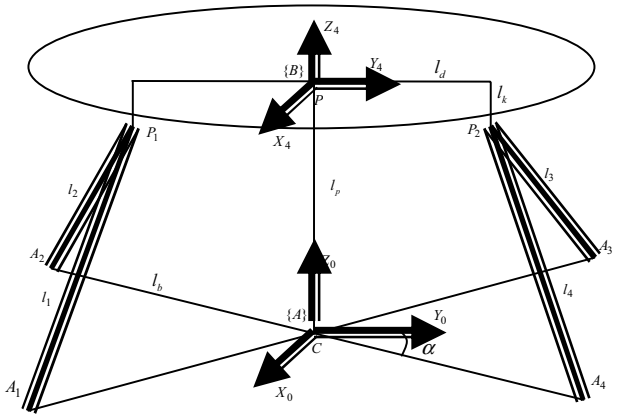

Figure 2. Geometric model for the hydraulic shoulder

$$U = U(\theta) \quad (12)$$

Hence, the Lagrange equations of motion can be rewritten as:

$$\frac{d}{dt}\left(\frac{\partial T(\theta,\dot{\theta})}{\partial \dot{\theta}}\right) - \frac{\partial T(\theta,\dot{\theta})}{\partial \theta} + \frac{\partial U(\theta)}{\partial \theta} = \tau_g \quad (13)$$

Using (13), the complete dynamic model of the hydraulic shoulder can be obtained as:

$$M(\theta)\ddot{\theta} + V(\theta,\dot{\theta}) + G(\theta) = \tau - \tau_e \quad (14)$$

Where the vectors $\theta, \dot{\theta}, \ddot{\theta}$ are the moving platform orientation angle, angular velocity and angular acceleration respectively, $M(\theta)$ is the 3×3 symmetric positive definite inertia matrix, $V(\theta,\dot{\theta})$ is the 3×1 vector of Coriolis and centrifugal torques, $G(\theta)$ is the 3×1 vector of gravitational torques, τ is the 3×1 vector of moving platform torques and τ_e is the 3×1 vector of external torques applied to the moving platform. Note that the control inputs to the dynamic equation is in fact the 4×1 vector of actuator forces, F, which is related to the moving platform torques, τ, by:

$$\tau = J^T(\theta) \cdot F \quad (15)$$

Where $J(\theta)$ is the 4×3 Jacobian matrix representing the relationship between the angular velocity of the moving platform and the vector of limb rates. The inertia Matrix $M(\theta)$ is directly given by the expression of the kinetic energy $T(\theta,\dot{\theta})$. The gravity term is obtained from the potential energy $U(\theta)$ by:

$$G(\theta) = \frac{\partial U(\theta)}{\partial \theta} \quad (16)$$

Finally, $V(\theta,\dot{\theta})$ which characterizes the Coriolis and centrifugal torques can be computed from the elements of the inertia matrix using the Christoffel symbols of the first type [11]. More details with this respect can be found in former studies by the authors [10,12].

V. Hydraulic Shoulder Impedance Control

A. Problem Definition

The objective of impedance control is to establish a desired dynamic relationship between the end-effector pose and the contact force, which is usually referred to as the target impedance. Let $\theta_d(t)$ be the desired trajectory of the end-

effector orientation angles. The impedance model or the target impedance is typically chosen as a linear second-order system just like mass-spring-damper dynamics such that:

$$M_D\ddot{e}_\theta + B_D\dot{e}_\theta + K_D e_\theta = \tau_e \quad (17)$$

Where M_D, B_D and K_D are constant positive definite 3×3 matrices of desired inertia, damping and stiffness respectively, τ_e is the external torque and e_θ is the orientation error defined as:

$$e_\theta = \theta_d - \theta \quad (18)$$

Regarding free motion, when there is no contact between the end-effector and the environment, e_θ reaches zero with proper choices of M_D, B_D and K_D. The desired transient response can be also satisfied choosing these matrices appropriately. In contact situation, the interaction of the end-effector with the environment is characterized by (17) in such a way that the external force is used for the impedance correction [5].

B. Impedance Control Design

There are two well known approaches to implement the impedance control concept, which are respectively referred to as torque-based and position-based impedance control [13]. In torque-based impedance control, torque information is assumed to be available, such that the impedance function can be implemented inside the control loop. In position-based impedance control, however, the impedance function is implemented outside the position loop. Thus the inner loop is controlled by the trajectory command input that is adjusted by position correction output from the impedance function of the outer loop. The first approach has been considered in the sequel.

1) Model-based Impedance Control Formulation

The torque-based impedance control law is chosen as:

$$\tau = u + V(\theta,\dot{\theta}) + G(\theta) + \tau_e \quad (19)$$

The closed loop behavior will satisfy the target impedance relationship choosing "u" as follows:

$$u = MD^{-1}\left\{D\ddot{\theta}_d + B\dot{e}_\theta + Ke_\theta - \tau_e\right\} \quad (20)$$

Substituting (19) and (20) into the dynamic equations (14) we obtain:

$$D(\theta)\ddot{e}_\theta + B\dot{e}_\theta + Ke_\theta = \tau_e \quad (21)$$

This is in fact in the form of the target impedance relationship. Figure (3) depicts the proposed torque-based impedance control structure.

2) Design Parameters Choice

The parameters of the impedance control scheme can be chosen regarding their effects on the steady state or transient responses. Assuming single axis design, the characteristic equation for the target impedance can be written as a standard second order system:

$$s^2 + 2\zeta\omega_n s + \omega_n^2 = 0 \quad (22)$$

Where:

$$\zeta = \frac{b_D}{2\sqrt{m_D k_D}},\ \omega_n = \sqrt{\frac{k_D}{m_D}} \quad (23)$$

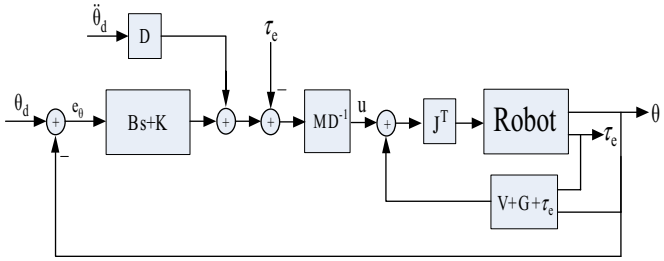

Figure 3. Model-Based Impedance Control Structure

The choice of impedance parameters m_D, b_D and k_D depends on the manipulation task objective in general, for example, when there is no contact with the environment the impedance control goal will be primarily position tracking in free space where no overshoot and oscillations is allowed in the transient response. However, in tasks like machine tooling where the end effector has contact with the environment, the impact should be small and the transient response should be without oscillations. In this case the impedance controller is set for both position and force tracking. Typically, large choice of m_D will result in large impact to the environment. For slow response without vibration large b_D should be selected. Also, position tracking corresponds to large values of stiffness k_D. In other words, high stiffness is specified in directions where the environment is compliant and position accuracy is important, large values of b_D are specified when energy dissipation is required and m_D can be used to provide smoothing for the end effector response due to external contact [3].

VI. Simulation Results

In order to verify the performance of the proposed method, a simulation study is forwarded. Different cases were considered in the simulations. First the hydraulic shoulder was considered in free motion where the external torque is zero. In this case the effectiveness of impedance control for positioning objectives is examined. The desired trajectory of the end-effector is prescribed by a typical cubic trajectory, which considers a smooth motion specified in terms of a desired pose of the moving platform of the hydraulic shoulder. The sample trajectory is defined given the initial and final points and the time to reach the final point, using common path planning routine developed for robotic manipulators. Target impedance model parameters were selected using the guidelines given in the previous section. The position tracking of the moving platform orientation angles are shown in figure 4. It can be seen that although the controller is designed for an impedance regulation, the closed loop yields to a suitable position-tracking capability. The error dynamics is also shown in figure 5 by means of plotting the impedance variation. Impedance variation is calculated from the residual of both sides of equation 21, which in this case in absence of any external force, illustrated the dynamics of the position tracking error, and the interaction among different channels.

In the second case, the manipulator is simulated while a contact release interaction to the environment is considered. This interaction is simulated with three pulse torques in three different axis applied as the external torque input at time *t=6 sec* and released at *t=11 sec.* As shown in figure 8, the amplitude of the torque pulse signal in *x* direction is selected twice as that for *y* and *z* direction, for the sake of comparison.

The results of position tracking, the tracking error and the impedance torque variations are depicted in figures 6, 7 and 8, respectively. In this case the impedance controller gain are selected as elaborated in previous section to reach to a desired second order dynamics with natural frequency ω_n=4Hz, and damping ratio ξ=0.5. As it is seen in figures 6 and 7, the controller is capable of regulating the positions, in presence of the contact force, with the desired impedance characteristics. The impedance error shown in figure 8 illustrates the dynamic relation between the contact force and moving platform position, and verifies the capability of the controller to preserve the desired impedance characteristics of the system, and regulation of the impedance error at steady state both at contact and release instances. The results show the effectiveness of the controller to impose the desired contact dynamics to the robot, despite the nonlinear characteristics of its dynamics.

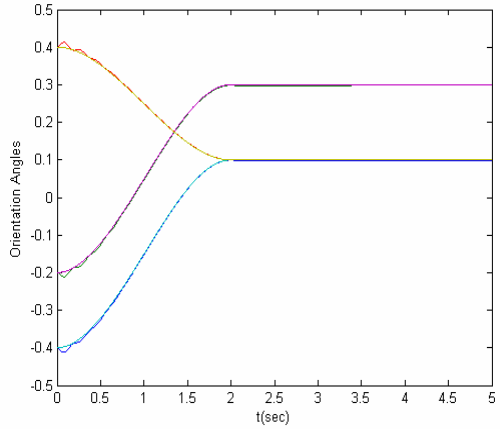

Figure 4. Trajectory tracking in free motion

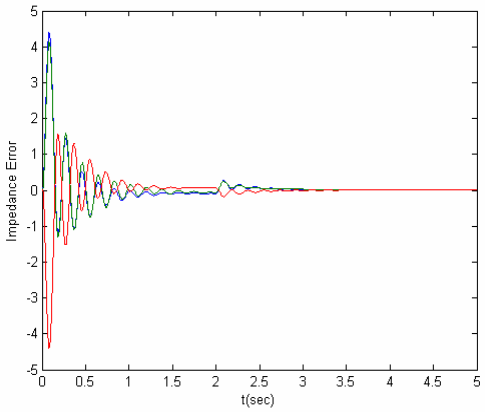

Figure 5. Impedance variations in free motion

VII. Conclusions

In this paper, kinematic analysis and dynamic modeling of a three DOF redundant parallel manipulator has been presented. A model-based impedance control structure has been designed for this manipulator in order to introduce the capability of interactions with environment. The impedance controller objective and the proposed topology is discussed and selection guides for controller gain are given. A simulation study has been carried out to test the effectiveness of the proposed method which showed the ability of the proposed impedance control scheme to combine high efficiency of position tracking in free motion and impedance adjustment of the robot in contact-release situation. It is shown through the simulation study that despite the nonlinear dynamics of the manipulator, it is completely plausible to introduce a linear dynamic model for the robot interacting with the environment, whose characteristics can be regulated by means of the controller parameters. In practice, however, there are always uncertainties in the manipulator dynamic model so the ideal target impedance model is not satisfied in general. Therefore, a robust impedance control method is necessary to compensate for the disturbances due to the uncertainties, which is the subject of our developing research.

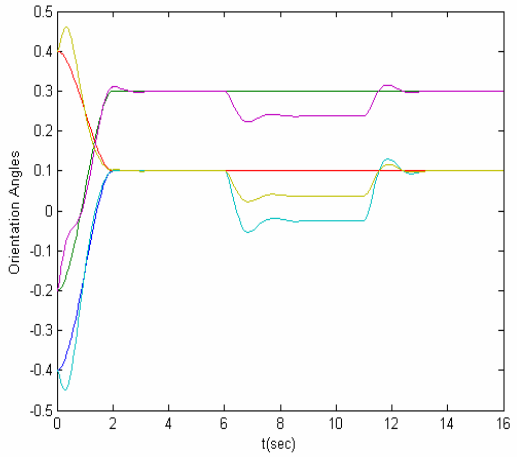

Figure 6. Trajectory tracking in contact-release to the environment; ω_n=4Hz, ξ=0.5

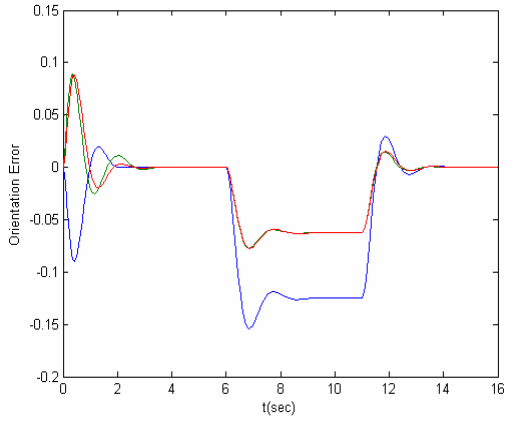

Figure 7. Tracking error in contact-release release to the environment; ω_n=4Hz, ξ=0.5

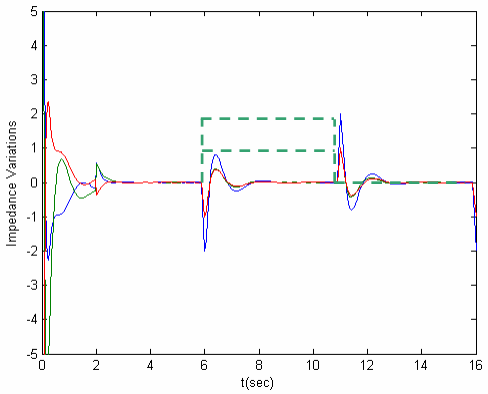

Figure 8. Impedance variations in contact-release release to the environment; ω_n=4Hz, ξ=0.5

REFERENCES

[1] J.P. Merlet, Still a long way to go on the road for parallel mechanisms, ASME 2002 DETC Conference, Montreal, Canada, 2002.

[2] J.P. Merlet, Parallel Robots: Open problems, In 9th Int'l. Symp. of Robotics Research, Snowbird, 9-12 October 1999.

[3] D. A. Lawrence, Impedance control stability properties in common implementations, in PROC. IEEE Int. Conf. Robotics and Automation, 1988, pp. 1185-1190.

[4] N. Hogan, Impedance control: an approach to manipulation, ASME Journal of Dynamic Systems, Measurement, and Control, vol. 107, pp. 1-24, 1985.

[5] Chiaverini, S.; Siciliano, B.; Villani,L.; A survey of robot interaction control schemes with experimental comparison, Mechatronics, IEEE/ASME Transactions, vol. 4, Issue 3, sept. 1999, 273-285.

[6] S. Joshi and L.W. Tsai, A comparison study of two 3-DOF parallel manipulators: One with three and the other with four supporting limbs, IEEE Trans. On Robotics & Automation, vol. 19, No. 2, April 2003, 200-209.

[7] E. D. Fasse and C.M. Gosselin, On the Spatial Impedance Control of Gough-Stewart Platforms, in PROC. IEEE Int. Conf. Robotics and Automation, 1998, pp. 1749-11754.

[8] V.Hayward, Design of a hydraulic robot shoulder based on a combinatorial mechanism, Experimental Robotics III: The 3rd Int'l Symposium, Japan Oct. 1994. Lecture Notes in Control & Information Sciences, Springer-Verlag, 297-310.

[9] H. Sadjadian and H.D. Taghirad, Numerical Methods for Computing the Forward Kinematics of a Redundant Parallel Manipulator, IEEE Conf. on Mechatronics and Robotics, Aachen, Germany, Sept. 2004, 557-562.

[10] H. Sadjadian and H.D. Taghirad, Kinematic and Singularity Analysis of the Hydraulic Shoulder: A 3-DOF Redundant Parallel Manipulator, The International Conference on Informatics in Control, Automation and Robotics, pp 125-131, Barcelona, Spain, Sept. 05.

[11] L. Sciavicco, B. Siciliano, Modeling and Control of Robot Manipulators, (2nd Ed.), Springer-Verlag, London, UK, 2000.

[12] H.D. Taghirad and S. Gholampour, Robust position control of hydraulic robotic shoulder, In the Proceedings of the 12th International Conference on Electrical Engineering, pp 286-291, May 2004, Mashad.

[13] S. Jung and T.C. Hsia, Neural Network Impedance Force Control of Robot Manipulator, IEEE transaction on Industrial Electronics, vol. 45, No. 3, June 1998, pp 451-461.